Partial-Measurement Backaction and Nonclassical Weak Values in a Superconducting Circuit

J. P. Groen,[1] D. Ristè,[1] L. Tornberg,[2] J. Cramer,[1] P. C. de Groot,[1,3] T. Picot,[1,4] G. Johansson,[2] and L. DiCarlo[1]

[1]*Kavli Institute of Nanoscience, Delft University of Technology, P.O. Box 5046, 2600 GA Delft, The Netherlands*
[2]*Microtechnology and Nanoscience, MC2, Chalmers University of Technology, SE-412 96 Goteborg, Sweden*
[3]*Max Planck Institute for Quantum Optics, Garching 85748 Munich, Germany*
[4]*Laboratory of Solid-State Physics and Magnetism, KU Leuven, Celestijnenlaan 200D, 3001 Leuven, Belgium*

(Received 21 February 2013; revised manuscript received 29 June 2013; published 29 August 2013)

We realize indirect partial measurement of a transmon qubit in circuit quantum electrodynamics by interaction with an ancilla qubit and projective ancilla measurement with a dedicated readout resonator. Accurate control of the interaction and ancilla measurement basis allows tailoring the measurement strength and operator. The tradeoff between measurement strength and qubit backaction is characterized through the distortion of a qubit Rabi oscillation imposed by ancilla measurement in different bases. Combining partial and projective qubit measurements, we provide the solid-state demonstration of the correspondence between a nonclassical weak value and the violation of a Leggett-Garg inequality.

DOI: 10.1103/PhysRevLett.111.090506 PACS numbers: 03.67.Lx, 42.50.Dv, 42.50.Pq, 85.25.−j

Quantum measurement involves a fundamental tradeoff between information gain and disturbance of the measured system that is traceable to uncertainty relations [1]. The backaction, or kickback, is a nonunitary process that depends on the measurement result and premeasurement system state. Thought experiments in the 1980s unveiled paradoxes [2–4] where the backaction of multiple measurements of one system puts quantum mechanics at odds with macrorealism (MAR) [2], a set of postulates distilling our common assumptions about the macroscopic world. Steady developments in the control of single quantum systems have opened the road to testing these paradoxes with photons [5–9], superconducting circuits [10], and semiconductor spins [11–13].

The Leggett-Garg inequality (LGI), for example, investigates the impact of backaction on the correlations between sequential measurements of one system [2,14]. A violation of the inequality certifies the failure of MAR to describe the system behavior. Although the original test called for multiple configurations of pairs of strong measurements, a generalization of the LGI using partial measurements requires only one configuration [15,16]. The first demonstration of LGI violations, by Palacios-Laloy *et al.* [10], used continuous weak measurement of a superconducting qubit. Further demonstrations followed using discrete measurements in photonic [7,8] and semiconductor-spin [12] systems. A second paradox is the nonclassicality of weak values, i.e., averages of a partial measurement conditioned on the result of a subsequent projective measurement [3]. These values are termed nonclassical when they lie outside the eigenspectrum of the weak measurement observable. Williams and Jordan [17] predicted an intriguing correspondence between nonclassical weak values (NCWVs) and the violation of generalized LGIs, first observed by Goggin *et al.* [7] using a photonic system.

Moving beyond fundamental investigation, the emergent field of quantum feedback control [18] balances the tradeoff between information gain and backaction. Applications requiring controllable measurement strength can be found in quantum error correction [19], qubit stabilization [20,21], and state discrimination [22]. A variable-strength measurement was first demonstrated in superconducting circuits using a Josephson phase qubit [23]. Although destructive for the qubit for one of two measurement outcomes, the method allowed probabilistic wave function uncollapse [24] by two sequential partial measurements, firmly demonstrating that backaction is phase coherent [25]. Recently [26], partial measurement of a transmon qubit was realized in circuit quantum electrodynamics (cQED) [27,28] by weakly probing transmission through a coupled cavity.

In this Letter, we demonstrate a nondestructive, variable-strength measurement of a transmon qubit. The measurement is based on controlled interaction with an ancilla qubit and projective ancilla measurement [Fig. 1(b)]. The key advantage of this indirect measurement is the possibility to accurately tailor the measurement by control of the interaction step and choice of ancilla measurement basis. The kickback of variable-strength measurements on the qubit is investigated by conditioning qubit measurements on the result of ancilla measurements in different bases, showing close agreement with theory. Combining partial and projective measurements, we realize the experiment of Ref. [7] and demonstrate the correspondence between NCWVs and LGI violations for the first time in a solid-state setting.

Our cQED device (Supplemental Material [29]) consists of two transmon qubits (Q_1 and Q_2) coupled jointly to a bus resonator (B) and separately to dedicated resonators (H_1 and H_2) [Fig. 1(a)]. Flux-bias lines allow the individual tuning of qubit transitions and resonant swapping of

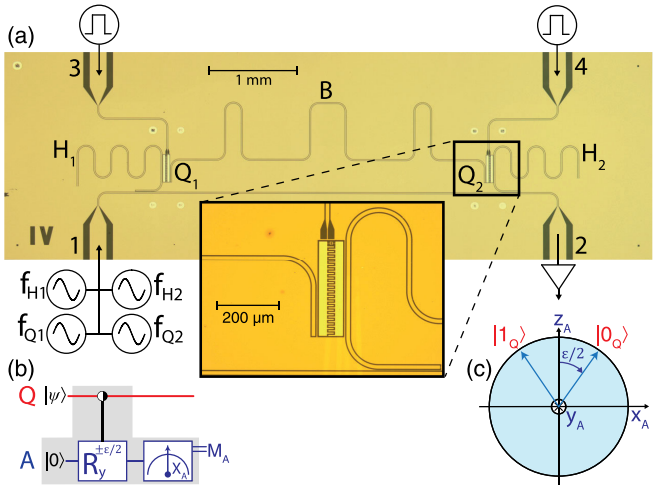

FIG. 1 (color online). (a) Two-transmon, three-resonator cQED processor. Resonators H_1 and H_2 allow individual readout of qubits Q_1 and Q_2 via a common feedline. A resonator bus B (single-photon quality factor 210 000) couples to both qubits. Local flux-bias lines (ports 3 and 4) allow independent tuning of qubit transition frequencies with ~1 GHz bandwidth [37]. (b) Scheme for two-step indirect measurement of one qubit (Q) through partial entanglement with an ancilla qubit (A) followed by projective measurement of A. (c) Bloch-sphere illustration of the evolution of A during the interaction step, for Q in $|0_Q\rangle$ and $|1_Q\rangle$.

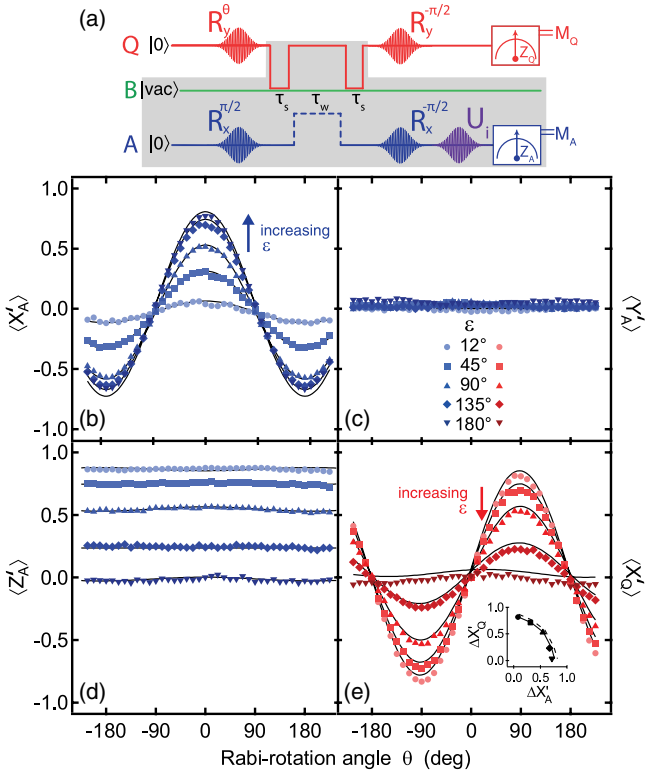

FIG. 2 (color online). (a) Pulse sequence realizing and testing the indirect measurement [Fig. 1(b)] of qubit $Q = Q_1$ with ancilla $A = Q_2$. Q is first prepared in state $|\theta\rangle = \cos(\theta/2)|0_Q\rangle + \sin(\theta/2)|1_Q\rangle$. [(b)–(d)] Ensemble-averaged ancilla measurement in the (b) X_A, (c) Y_A, and (d) Z_A bases, achieved using premeasurement rotation $U_i = R_{y_A}(-\pi/2)$, $R_{x_A}(\pi/2)$ and identity, respectively. In the experiment, $R_{x_A}(-\pi/2)$ and U_i are compiled into one rotation to reduce the effects of qubit decoherence. (e) Partial-measurement backaction reduces the contrast in the final projective measurement of Q. Ideally, $\langle X'_Q\rangle = \langle Z_Q\rangle\cos(\epsilon/2)$, independent of M_A basis (X_A here, see the Supplemental Material [29] for the three bases). Inset: Parametric plot of oscillation amplitudes $\Delta X'_Q$ and $\Delta X'_A$. $\Delta X'_Q$ ($\Delta X'_A$) decreases (increases) as ϵ increases in the range [0°,180°]. Solid (dashed) curves correspond to the model with (without) decoherence during the gate.

excitations between either qubit and B. All microwave pulses for individual qubit control and readout are applied through a common feedline coupled to H_1 and H_2. Projective readout of Q_1 (Q_2) is performed by measuring feedline transmission at the resonance frequency of H_1 (H_2) achieving 85% (94%) single-shot fidelity (see Fig. S4 of the Supplemental Material [29] for more device details).

The interaction step in the indirect measurement is a y rotation of the ancilla ($A = Q_2$) by $\pm\epsilon/2$, with positive (negative) sign for $Q = Q_1$ in $|0_Q\rangle$ ($|1_Q\rangle$) [Fig. 1(c)]. The angle ϵ sets the degree of entanglement between Q and A and therefore the measurement strength. Note that $\epsilon = 180°$ makes the measurement projective, as in this case A evolves to orthogonal states for $|0_Q\rangle$ and $|1_Q\rangle$, maximizing the entanglement. The Q-dependent y rotation of A is achieved by dressing a controlled-z rotation with pre- and postrotations on A [Fig. 2(a)]. The controlled-z rotation is a three-step process: a resonant swap transferring the state of Q to B, a photon-controlled z rotation of A, and a resonant swap from B back to Q. The acquired two-qubit phase ϵ is calibrated by varying the wait time τ_w and the detuning between A and B (Supplemental Material [29]).

We characterize the interaction step by performing individual measurements of both Q and A after the interaction, with Q initially prepared in the superposition state $|\theta_Q\rangle = \cos(\theta/2)|0_Q\rangle + \sin(\theta/2)|1_Q\rangle$ and A and B in the ground state. As in this part we focus purely on the interaction, we correct for readout errors of A and Q using standard calibration procedures (Supplemental Material [29]) [30]. Ideally, $\langle X'_A\rangle = \langle Z_Q\rangle\sin(\epsilon/2)$, $\langle Y'_A\rangle = 0$, and $\langle Z'_A\rangle = \cos(\epsilon/2)$ [(un-) primed notation denotes the (pre-) postinteraction state, and X_i, Y_i, and Z_i are the Pauli operators acting on i]. These dependencies are well reproduced in the data for all choices of ϵ [Figs. 2(b)–2(d)]. Measuring in either the Y_A or Z_A basis yields no information about the initial state of Q, as expected. We also measure the postinteraction contrast $\Delta X'_Q$ of the Q Rabi oscillation [Fig. 2(e)] and compare it to the contrast $\Delta X'_A$ of the interaction-induced oscillation in A. As ϵ increases, $\Delta X'_Q$ decreases while $\Delta X'_A$ increases. Ideally, the quadrature sum $\sqrt{(\Delta X'_Q)^2 + (\Delta X'_A)^2} = 1$ for any ϵ. We observe a monotonic decrease from 0.82 at $\epsilon = 12°$ to 0.72 at

$\epsilon = 180°$ [Fig. 2(e) inset]. This decrease is reproduced by a master equation simulation that includes 4% residual excitation and measured decoherence rates for each element (Supplemental Material [29]).

We now investigate the quantum kickback of the indirect measurement by measuring $\langle X'_Q \rangle$ conditioned on the result of ancilla measurement $M_A = \pm 1$ in different bases. Results in Fig. 3 show the partial-measurement-induced

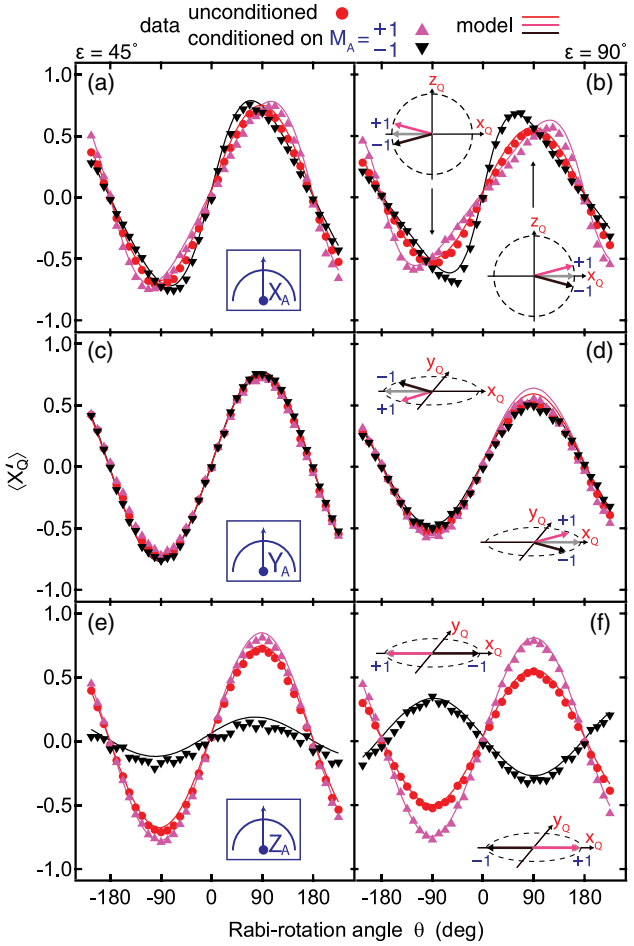

FIG. 3 (color online). Partial-measurement kickback. The kickback on qubit Q induced by partial measurement depends on the interaction strength ϵ, the ancilla measurement basis, and measurement result M_A. Left and right panels correspond to $\epsilon = 45°$ and 90°, respectively. [(a),(b)] Conditioning on the result M_A of ancilla measurement in the X_A basis reveals distorted Rabi oscillations of Q. A positive (negative) result retards (advances) the oscillation for $\theta \in [0°, 180°]$ and advances (retards) it for $\theta \in [180°, 360°]$. [(c),(d)] Distortions for measurement in the Y_A basis. In this case, the kickback is a z rotation by $\pm\epsilon/2$, causing an identical reduction of contrast in the conditioned Rabi oscillations. [(e),(f)] Distortions for measurement in the Z_A basis. Ideally, $M_A = +1$ has no kickback on Q, whereas $M_A = -1$ causes a z rotation of π. To extract $\langle X'_Q \rangle$, we correct for readout errors of Q using standard calibration procedures [29,30]. The difference in contrast for $\langle X'_Q \rangle$ for $M_A \pm 1$ is due to asymmetric readout errors of A (Supplemental Material [29]).

distortion of a Rabi oscillation of Q for $\epsilon = 45°$ and 90° (see the Supplemental Material [29] for other ϵ values) and ancilla-measurement bases X_A, Y_A, and Z_A. For X_A, outcome $M_A = \pm 1$ kicks Q toward the north (south) pole of the Bloch sphere. Ideally, the Bloch vector polar angle transforms as $\theta \rightarrow \theta'$, with $\tan(\theta'/2) = \tan(\theta/2)[1 - M_A \tan(\epsilon/4)]/[1 + M_A \tan(\epsilon/4)]$, while the azimuthal angle is conserved. When measuring Y_A, conditioning does not distort the Rabi oscillation. This is because the kickback of $M_A = \pm 1$ is a z rotation of Q by $\pm\epsilon/2$, leading to the same x projection. Conditioning on a Z_A measurement produces the most striking difference: while $M_A = +1$ imposes no kickback, $M_A = -1$ imposes a z rotation of π. Ideally, both curves are unit-amplitude sinusoids with opposite phase, independent of ϵ. However, for $\epsilon = 45°$, the $M_A = -1$ set is dominated by false negatives. As ϵ increases, true $M_A = -1$ counts become more abundant and we observe the expected sign reversal in the conditioned curve with $\epsilon = 90°$. Note that despite the difference in conditioned curves for the different A measurement bases, the three unconditioned curves are nearly identical. This is consistent with the expectation that measurement-induced dephasing is independent of the ancilla measurement basis [18].

As a benchmark of the complete indirect-measurement scheme, we extract quantum efficiencies η_i characterizing the loss of quantum information [31] for measurement outcome $M_A = i$

$$\eta_i \equiv \left(\frac{\langle X'_Q \rangle^2 + \langle Y'_Q \rangle^2}{1 - \langle Z'_Q \rangle^2} \right)^{1/2}_{|M_A = i} \Big/ \left(\frac{\langle X_Q \rangle^2 + \langle Y_Q \rangle^2}{1 - \langle Z_Q \rangle^2} \right)^{1/2}.$$

Loss originates in the single-shot readout infidelity of A, the residual excitation in A and B, and decoherence of Q, A, and B during the interaction. Without decoherence, η_i would be independent of input qubit state (see the Supplemental Material [29] for full expressions). Using the calibrated measurement and gate infidelities and residual excitations, we estimate $\eta_{\pm 1} = 0.94(0.94)$ at $\epsilon = 45°$ and 0.85(0.83) at 90°. Including decoherence and averaging over the qubit Bloch sphere, we estimate $\bar{\eta}_{\pm 1} = 0.77(0.71)$ at $\epsilon = 45°$ and 0.69(0.60) at 90°.

Finally, we combine the abilities to perform partial and projective measurements to observe NCWVs, detect LGI violations, and demonstrate their correspondence [7,17] (Fig. 4). The partial measurement of $Q = Q_2$ is performed via $A = Q_1$ in basis X_A and the projective measurement in basis X_Q. We measure the partial-measurement average conditioned on the digitized strong-measurement result $M_Q = -1$,

$$W_{\mathrm{m}} \equiv \langle \tilde{M}_A \rangle_{|M_Q = -1},$$

where M_A is rescaled to $\tilde{M}_A \equiv (M_A - m_{\mathrm{off}})/m_{\mathrm{pk}}$ so that $\langle \tilde{M}_A \rangle = \pm 1$ for initial preparation of Q in $|0_Q\rangle(|1_Q\rangle)$

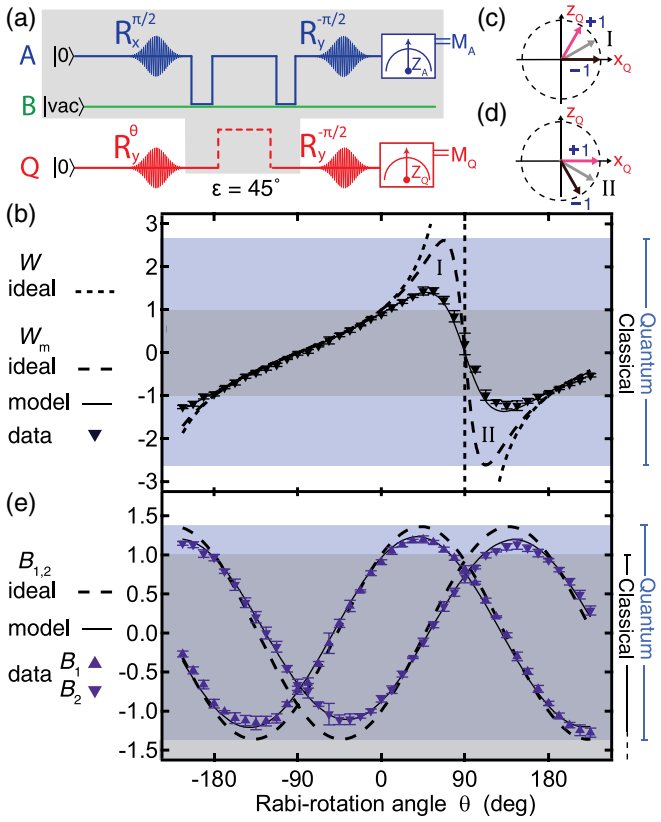

FIG. 4 (color online). Observation of nonclassical weak values and Leggett-Garg inequality violations (measurement strength $\epsilon = 45°$). (a) Pulse sequence. Note that qubit roles are swapped ($Q = Q_2$ and $A = Q_1$) compared to previous figures in order to minimize errors when conditioning on $M_Q = \pm 1$. (b) Dependence of modified weak value W_m (see text for definition and normalization procedure) on Q-rotation angle θ. The MAR bound $|W_m| \leq 1$ is amply exceeded. From the quantum perspective, the extrema in W_m at I and II can be understood using the Bloch spheres in (c) and (d), respectively. Ideally, at I (II), the $M_A = -1(+1)$ kickback aligns Q with the $+x_Q$ axis, perfectly correlating $M_Q = -1$ with $M_A = +1(-1)$. (e) Measured averaged Leggett-Garg operators $B_{1,2}$ defined in text. One of the inequalities $B_{1,2} \leq 1$ is violated whenever nonclassical W_m is observed.

[7,8,32]. Whereas MAR constrains $|W_m| \leq 1$, the ideal quantum setting (perfect preparation, interaction, and measurements) allows $|W_m| = \csc(\epsilon/2)$. This can be understood by noting that under these conditions $m_{pk} = \sin(\epsilon/2)$ and $m_{off} = 0$, while $M_A = +1$ [Fig. 4(c)] ($M_A = -1$ [Fig. 4(d)]) always when Q is prepared in $|(\pi \mp \epsilon)/2_Q\rangle$ and $M_Q = -1$ (full derivation given in the Supplemental Material [29]). In experiment, imperfect preparation and readout of Q will lower $|W_m|$ but not those of A (due to the scaling procedure). We call W_m a modified weak value because it differs in the ideal quantum setting from the standard definition [3] of the weak value W of operator Z_Q between initial state $|\theta_Q\rangle$ and final state $|-\pi/2_Q\rangle$,

$$W \equiv \frac{\langle -\pi/2_Q|Z_Q|\theta_Q\rangle}{\langle -\pi/2_Q|\theta_Q\rangle}.$$

Specifically, the finite range ($M_A \in \{-1, 1\}$) of ancilla-based measurement regularizes W_m near $\theta = \pi/2$ (Supplemental Material [29]) [33], where W diverges [Fig. 4(b)].

In parallel, we consider the generalized Leggett-Garg correlation function $\langle M_1\rangle - \langle M_1 M_2\rangle + \langle M_2\rangle$ with partial measurement M_1 and strong measurement M_2 [16,17]. In the original proposal [2], a first measurement M_0 had the function of initializing the system in a known state. Similarly to Refs. [7,9], we omit M_0 and instead rely on state initialization by relaxation toward $|0_Q\rangle$. From the family of generalized LGIs that can be constructed by changing the sign of M_1 or M_2, we focus on

$$B_1 \equiv \langle \tilde{M}_A\rangle - \langle \tilde{M}_A M_Q\rangle + \langle M_Q\rangle,$$
$$B_2 \equiv -\langle \tilde{M}_A\rangle + \langle \tilde{M}_A M_Q\rangle + \langle M_Q\rangle,$$

where $\tilde{M}_A = M_1$ and $M_Q = M_2$. While the MAR postulates bound $-3 \leq B_{1,2} \leq 1$, for the sequence in Fig. 4(a) the ideal quantum setting sets the range $|B_{1,2}| \leq \sqrt{(\cos(\epsilon) + 3)/2}$. Similarly to $|W_m|$, $|B_{1,2}|$ will be reduced by imperfect preparation and readout of Q, but not of A.

We demonstrate a smooth crossing of MAR bounds for W_m and $B_{1,2}$ by performing the experiment in Fig. 4(a) over a range of initial qubit states $|\theta_Q\rangle$. We observe a maximum W_m of 1.44 ± 0.07. In turn, B_1 and B_2 peak at 1.20 ± 0.04 and 1.14 ± 0.06, respectively. The data clearly show that one of the two LGIs is violated whenever W_m is nonclassical. This observation matches the prediction of Ref. [17] and the first experimental test in Ref. [7] using photons. The correspondence becomes the more interesting upon noting that $B_{1,2}$ averages all measurements while W_m uses only the postselected fraction for which $M_Q = -1$.

In conclusion, we have realized an indirect measurement of a transmon qubit with high quantum efficiency and tunable measurement strength. Our scheme consists of a partially entangling interaction between the qubit and an ancilla, followed by projective ancilla measurement using a dedicated resonator. We have measured the kickback of such measurements on the qubit as a function of interaction strength and ancilla measurement basis, finding close agreement with theory. Nonclassical weak values are observed upon conditioning ancilla measurements on the outcome of a projective measurement of the qubit. Their predicted correspondence with LGI violations is demonstrated for the first time in a solid-state system. The combination of high-quality factor bus, individual readout resonators, and feedline here demonstrated constitutes a scalable architecture [34] with frequency-multiplexable single-qubit control and readout [35]. Future experiments will target the realization of the ancilla-based 4-qubit

parity measurement needed for surface-code quantum error correction [36].

We thank D. Thoen and T. M. Klapwijk for NbTiN thin films, A. Frisk Kockum for contributions to theoretical modeling, and S. Ashhab, Ya. M. Blanter, M. H. Devoret, M. Dukalski, G. Haack, and R. Hanson for helpful discussions. We acknowledge funding from the Dutch Organization for Fundamental Research on Matter (FOM), the Netherlands Organization for Scientific Research (NWO, VIDI scheme), the EU FP7 project SOLID, and the Swedish Research Council.

[1] V. B. Braginsky and F. Y. Khalili, *Quantum Measurement* (Cambridge University Press, Cambridge, England, 1995).
[2] A. J. Leggett and A. Garg, Phys. Rev. Lett. **54**, 857 (1985).
[3] Y. Aharonov, D. Z. Albert, and L. Vaidman, Phys. Rev. Lett. **60**, 1351 (1988).
[4] Y. Aharonov and L. Vaidman, J. Phys. A **24**, 2315 (1991).
[5] K. Resch, J. Lundeen, and A. Steinberg, Phys. Lett. A **324**, 125 (2004).
[6] G. J. Pryde, J. L. O'Brien, A. G. White, T. C. Ralph, and H. M. Wiseman, Phys. Rev. Lett. **94**, 220405 (2005).
[7] M. E. Goggin, M. P. Almeida, M. Barbieri, B. P. Lanyon, J. L. O'Brien, A. G. White, and G. J. Pryde, Proc. Natl. Acad. Sci. U.S.A. **108**, 1256 (2011).
[8] J. Dressel, C. J. Broadbent, J. C. Howell, and A. N. Jordan, Phys. Rev. Lett. **106**, 040402 (2011).
[9] Y. Suzuki, M. Iinuma, and H. F. Hofmann, New J. Phys. **14**, 103022 (2012).
[10] A. Palacios-Laloy, F. Mallet, F. Nguyen, P. Bertet, D. Vion, D. Esteve, and A. N. Korotkov, Nat. Phys. **6**, 442 (2010).
[11] G. Waldherr, P. Neumann, S. F. Huelga, F. Jelezko, and J. Wrachtrup, Phys. Rev. Lett. **107**, 090401 (2011).
[12] G. C. Knee *et al.*, Nat. Commun. **3**, 606 (2012).
[13] R. E. George, L. M. Robledo, O. J. E. Maroney, M. S. Blok, H. Bernien, M. L. Markham, D. J. Twitchen, J. J. L. Morton, G. A. D. Briggs, and R. Hanson, Proc. Natl. Acad. Sci. U.S.A. **110**, 3777 (2013).
[14] C. Emary, N. Lambert, and F. Nori, arXiv:1304.5133.
[15] R. Ruskov, A. N. Korotkov, and A. Mizel, Phys. Rev. Lett. **96**, 200404 (2006).
[16] A. N. Jordan, A. N. Korotkov, and M. Büttiker, Phys. Rev. Lett. **97**, 026805 (2006).
[17] N. S. Williams and A. N. Jordan, Phys. Rev. Lett. **100**, 026804 (2008); **103**, 089902(E) (2009).
[18] H. M. Wiseman and G. J. Milburn, *Quantum Measurement and Control* (Cambridge University Press, Cambridge, 2009).
[19] A. M. Brańczyk, P. E. M. F. Mendonça, A. Gilchrist, A. C. Doherty, and S. D. Bartlett, Phys. Rev. A **75**, 012329 (2007).
[20] J. Wang and H. M. Wiseman, Phys. Rev. A **64**, 063810 (2001).
[21] R. Vijay, C. Macklin, D. H. Slichter, K. W. Murch, R. Naik, N. Koroktov, and I. Siddiqi, Nature (London) **490**, 77 (2012).
[22] G. Waldherr, A. C. Dada, P. Neumann, F. Jelezko, E. Andersson, and J. Wrachtrup, Phys. Rev. Lett. **109**, 180501 (2012).
[23] N. Katz *et al.*, Science **312**, 1498 (2006).
[24] A. N. Korotkov and A. N. Jordan, Phys. Rev. Lett. **97**, 166805 (2006).
[25] N. Katz *et al.*, Phys. Rev. Lett. **101**, 200401 (2008).
[26] M. Hatridge *et al.*, Science **339**, 178 (2013).
[27] A. Wallraff, D. I. Schuster, A. Blais, L. Frunzio, R.-S. Huang, J. Majer, S. Kumar, S. M. Girvin, and R. J. Schoelkopf, Nature (London) **431**, 162 (2004).
[28] A. Blais, R.-S. Huang, A. Wallraff, S. M. Girvin, and R. J. Schoelkopf, Phys. Rev. A **69**, 062320 (2004).
[29] See Supplemental Material at http://link.aps.org/supplemental/10.1103/PhysRevLett.111.090506 for device details, experimental methods, extended results and modeling.
[30] A. Wallraff, D. I. Schuster, A. Blais, L. Frunzio, J. Majer, M. H. Devoret, S. M. Girvin, and R. J. Schoelkopf, Phys. Rev. Lett. **95**, 060501 (2005).
[31] A. N. Korotkov, Phys. Rev. B **78**, 174512 (2008).
[32] We extract m_{pk} and m_{off} from the best sinusoidal fit of $\langle M_A \rangle$ as a function of the prepared state $|\theta_Q\rangle$ and accounting for the calibrated 4% residual excitation of Q (Supplemental Material [29]).
[33] S. Wu and K. Mølmer, Phys. Lett. A **374**, 34 (2009).
[34] During bring up of this device, two-qubit algorithms [37] were performed achieving a quantum speedup similar to that of Ref. [38]. See J. Cramer, master's thesis, Delft University of Technology, 2012.
[35] Y. Chen *et al.*, Appl. Phys. Lett. **101**, 182601 (2012).
[36] A. G. Fowler, M. Mariantoni, J. M. Martinis, and A. N. Cleland, Phys. Rev. A **86**, 032324 (2012).
[37] L. DiCarlo *et al.*, Nature (London) **460**, 240 (2009).
[38] A. Dewes, R. Lauro, F. R. Ong, V. Schmitt, P. Milman, P. Bertet, D. Vion, and D. Esteve, Phys. Rev. B **85**, 140503 (2012).